Best-fit Segmentation Created Using Flood-based Iterative Thinning

Adam Piórkowski[1]

AGH University of Science and Technology,
Department of Geoinfomatics and Applied Computer Science
A. Mickiewicza 30 Av., 30–059 Krakow, Poland
pioro@agh.edu.pl

Summary. Classical methods of segmentation that use binarization in the preprocessing stage often do not provide the precise delineation of the range of objects. For example, this might be useful for images of the corneal endothelium obtained with specular or confocal microscopy. This article presents a solution that makes it possible to adjust the course of the segmentation in the valleys between cells. The algorithm is a combination of iterative thinning and a watershed algorithm that works by the gradual removal of points with increasingly lower brightness levels. The article also contains examples of output images and quality tests[0].

Key words: segmentation, iterative thinning, corneal endothelium

1 Introduction

The segmentation of corneal endothelium images is a difficult issue due to the nature of the images obtained with confocal or specular microscopy. These images have a relatively high proportion of thermal noise, low contrast, and non-uniform luminance, all of which are qualities that prevent the use of algorithms such as the watershed algorithm. Instead, there are different methods to obtain binary images.

The authors in [12] propose the use of non-subsampled wavelet pyramid decomposition of lowpass regions. The pre-processing includes removal of non-uniform illumination and noise. Post processing includes dilatation, erosion, opening and closing operations, and finally thinning. Other method to deal with blown-out illumination areas is presented in [16]. Mahzoun et al. [13] propose using six convolution masks of size 9×9 that perform directional

[0] This is the manuscript of:

Piorkowski A.: Best-fit Segmentation Created Using Flood-based Iterative Thinning. Springer, AISC Vol. 525, pp 61–68, 2017

filtering (vertical, horizontal, left and right) and custom filtering (two 'tricorn' masks and binarization of the sum of outputs). In [9], a similar effective method is presented which assumes the use of four directional masks. These two approaches need thinning as the last step of segmentation. Sanches [21] uses scale-space filtering, especially Gaussian, to make use of the separability property of the Gaussian kernel, and unsharp masking. Adaptive thresholding and binarization are also used. Subsequently, skeletonization (thinning) is performed.

A custom method is presented in [15]. The authors propose a scissoring operator that separates cells in the binary image. The most advanced approaches use the active contour technique to obtain the shape of each cell in the image [1, 10], or artificial neuron networks with numerical filters designed for the border extraction problem [7].

2 The Problem of Imprecise Segmentation

Most of the presented approaches (even clinical programs) do not necessarily perform precise segmentation. The true shape of some cells is not precisely drawn (Fig. 1). This problem has been described in the literature [2, 18, 11, 14].

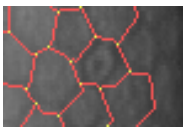

Fig. 1. A sample of imprecise segmentation.

2.1 Thinning

In all these approaches, a binary image is thinned. Iterative thinning is usually the gradual removal of points from all sides of objects [20]. When images of the corneal endothelium are binarized, a side effect of this approach is that the dividing line between the cells does not necessarily fall on the pits or valleys. Some dividing lines are located on the slopes of particular cells. Therefore, this does not make for a representative and repetitive segmentation as some of cell grid parameters are sensitive and can depend on the segmentation method. To ensure the objectivity and reproducibility of clinical parameters, the segmentation lines should obtained, as they ran at the bottom of valleys.

The lack of precision may occur during the thinning of the binary images that are the result of most of the presented algorithms. In the classic approach to thinning, iterative symmetrical cuts are made to binary images by deleting

points evenly on each side of the object to obtain a contour that is one pixel thick. This approach may cause the resulting contour not to cover the bottom of the valley (Fig. 2).

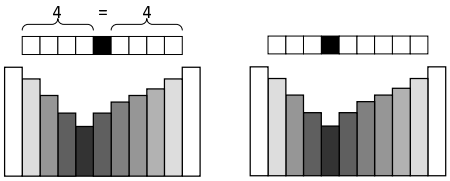

(a) Classic (b) Required

Fig. 2. Differences between classic and required thinning.

Thinning is usually carried out using a Hit-or-Miss algorithm with a set of carefully selected masks (Golay Alph.). In the present work, the set of masks described in Tab. 1 are used; each of them appears in orientations of 0°, 90° 180° and 270°.

$$\begin{bmatrix} X & 1 & 1 \\ 0 & 1 & 1 \\ 0 & 0 & X \end{bmatrix} \quad \begin{bmatrix} X & 1 & X \\ X & 1 & X \\ 0 & 0 & 0 \end{bmatrix} \quad \begin{bmatrix} X & X & 0 \\ 0 & 1 & 0 \\ 0 & 0 & 0 \end{bmatrix} \quad \begin{bmatrix} 0 & X & X \\ 0 & 1 & 0 \\ 0 & 0 & 0 \end{bmatrix}$$

Table 1. A set of masks for thinning

To solve the problem of imprecise thinning (imprecise segmentation) some approaches have been developed.

2.2 Adjusting the Valley Segmentation Courses

Very interesting solution to the problem of search segmentation best suited to valleys was presented by B. Selig et al. [22]. The method comprises two parts. In the first stage, the seeded watershed is applied many times with seeds placed randomly (stochastic watershed). The next step blurs the output with a Gaussian filter, which removes local minima, and finally a classic watershed is used. To evaluate the output, the mean gray values of source pixels under the segmentation line (MGV) are calculated.

A second approach is presented in [18], the first part of which determines the number of neighbors of less than or equal brightness to each image point in the input image. The second phase performs iterative thinning on the basis of the constructed neighborhood map (NMIT) [17]. Each of the 9 thinning iterations removes only points that correspond to values in the maps.

3 Flood-based Iterative Thinning Algorithm (FIT)

In order to solve the problem, a new algorithm is proposed which is a combination of a thinning algorithm and a watershed algorithm. This approach involves iterative thinning of binary images with reference to the source input image. Thinning iterations run in the same way as flooding in the watershed algorithm; in the case of dark valleys and bright objects in the source image, the iterations are carried out from the highest brightness (255 for 8 bit grayscale images) to the lowest brightness (0). In each iteration, only points of the binary image where the brightness in the source image is greater than or equal to the number of the iteration are processed. As a result, the highest points above and the lowest points below are removed, unless, of course, they match the thinning mask pattern. This method reduces the symmetrical thinning phenomenon; in its place, there is a solution most suited to the valleys in the image. A similar approach of thinning for grayscale images is presented in [4, 3]. The algorithm can be presented in the form of pseudo-code:

```
FOR level = 255 TO 0
    ThinPoints(segmentation) WHERE SourceImage[x,y] >= level
```

3.1 Improvement of Thinning

The resulting segmentation of the binary image might be not necessarily the best fit because the binary image could cover a slope, instead of the lowest parts of the valley. In this case, the proposed solution is a cyclical correction, based on dilation and iterative thinning. No more improvements are made when there are no more changes, or a looped cycle is detected.

3.2 Testing of Flood-based Iterative Thinning

Tests were carried out to assess a sample of segmentation quality. As a source data, the Endothelial Cell Alizarine Data Set was chosen [19]. It contains 30 corneal endothelium images and the corresponding manual segmentations.

Fig. 3(a) contains a fragment of the original image and manual seed (Fig. 3(b)) from the data set (No 4). The next figure (Fig. 3(c)) shows segmentation seed after dilatation. The drawings (Fig. 4) show a selection of iterative thinning stages for levels 140, 120, 100, 90, 80 and 60. It can be seen that this iterative thinning first removes points that cover the higher parts, and then deletes the lowest points.

A qualitative assessment of the proposed method is needed. For this purpose, a comparison of the original thinned segmentation and NMIT and FIT methods was prepared. Segmentation was corrected by performing iterative cycles of dilatation and modified thinning (Fig. 5). A description of the subsequent stage, including the differences between images and the mean gray value of segmentation (MGV), are presented in Table 2, which shows the results for the thinned original segmentation, improved by NMIT and FIT algorithms.

(a) original (b) segmentation seed (c) dilatated seed

Fig. 3. Input pictures.

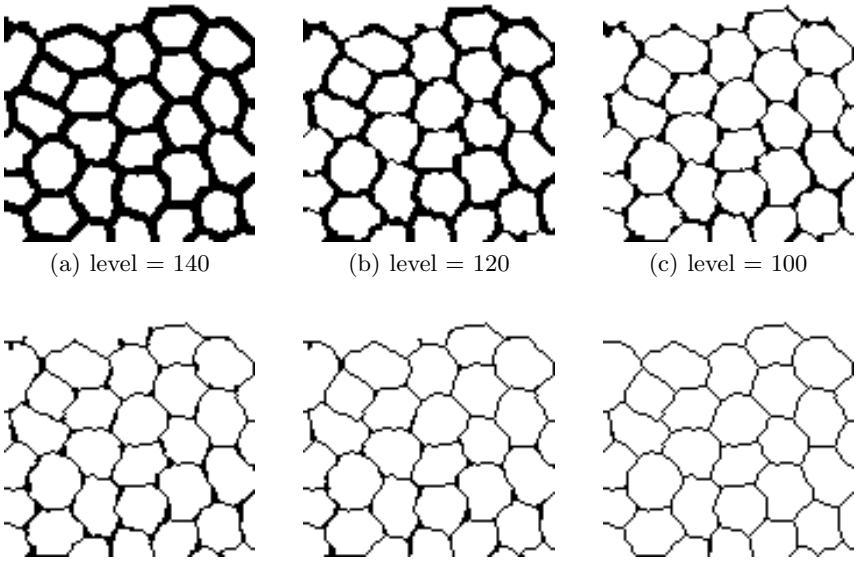

(a) level = 140 (b) level = 120 (c) level = 100

(d) level = 90 (e) level = 80 (f) level = 60

Fig. 4. Thinning iterations for selected levels.

Table 2. The performance of iterative thinnings.

	NMIT		FIT	
cycle	differences [px]	MGV	differences [px]	MGV
initial thinning		112.7477		112.7477
1	9587	109.4422	10152	109.2717
2	807	109.3556	467	109.2190
3	94	109.3536	0	109.2190
4	24	109.3413		
5	8	109.3363		
6	0	109.3363		

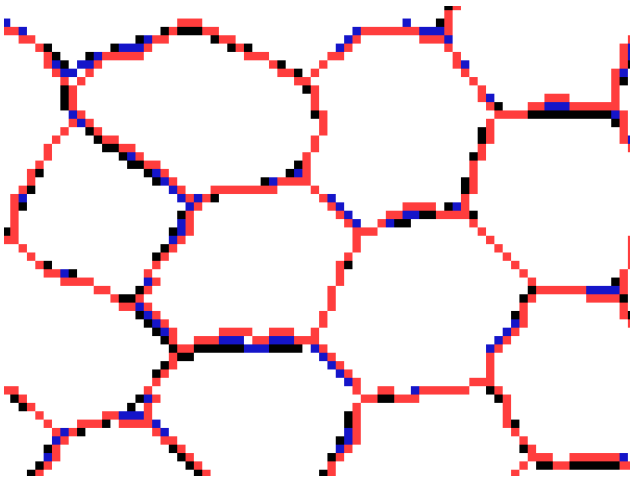

Fig. 5. Differences between segmentations obtained in subsequent dilatation and FIT thinning cycles; black - initial segmentation, blue (dark gray) - first cycle, red (light gray) - second cycle (final).

4 Conclusions

The presented algorithm matched the lines of segmentation to the source image fairly well. In addition, not only the optical effect Fig.6 can be recognized as the obtained mean gray value of segmentation was better for the FIT algorithm than the NMIT algorithm and classical thinning. Moreover, the number of cycles of dilatation and thinning was smaller. It can be concluded that the proposed algorithm performs solves the problem quite well. Further studies will focus on the quality of thinning compared to other methods (eg. FRSW) and the effects of the method for changing shape factors, eg. CV [5], H [6] and $CVSL$ [8].

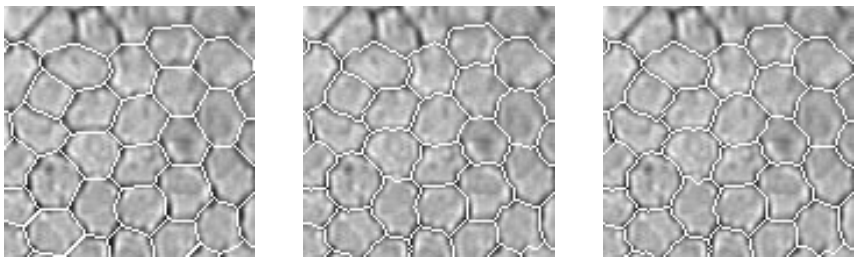

(a) Classic thinning (b) NMIT improvement (c) FIT improvement

Fig. 6. Input pictures with overlayed segmentation.

Acknowledgement

This work was financed by the AGH - University of Science and Technology, Faculty of Geology, Geophysics and Environmental Protection as a part of statutory project.

References

[1] Charłampowicz K, Reska D, Boldak C (2014) Automatic segmentation of corneal endothelial cells using active contours. Advances in Computer Science Research 11:47–60

[2] Cheung SW, Cho P (1998) Endothelial cell analysis using the Topcon SP-1000 non-contact specular microscope and IMAGEnet system. Clinical and Experimental Optometry 81(1):1–7

[3] Couprie M, Bezerra FN, Bertrand G (2001) Topological operators for grayscale image processing. Journal of Electronic Imaging 10(4):1003–1015

[4] Couprie M, Bezerra N, Bertrand G (2013) A parallel thinning algorithm for grayscale images. In: Discrete Geometry for Computer Imagery, Springer, pp 71–82

[5] Doughty M (1990) The ambiguous coefficient of variation: Polymegethism of the corneal endothelium and central corneal thickness. International Contact Lens Clinic 17(9-10)

[6] Doughty M (1992) Concerning the symmetry of the hexagonal cells of the corneal endothelium. Experimental eye research 55(1):145–154

[7] Foracchia M, Ruggeri A (2000) Cell contour detection in corneal endothelium in-vivo microscopy. In: Engineering in Medicine and Biology Society, 2000. Proceedings of the 22nd Annual International Conference of the IEEE, IEEE, vol 2, pp 1033–1035

[8] Gronkowska-Serafin J, Piorkowski A (2014) Corneal endothelial grid structure factor based on coefficient of variation of the cell sides lengths. In: Image Processing and Communications Challenges 5, Advances in Intelligent Systems and Computing, vol 233, Springer, pp 13–19

[9] Habrat K, Habrat M, Gronkowska-Serafin J, Piorkowski A (2016) Cell detection in corneal endothelial images using directional filters. In: Image Processing and Communications Challenges 7, Advances in Intelligent Systems and Computing, vol 389, Springer, pp 113–123

[10] Hachaj T, Ogiela MR (2014) Application of centerline detection and deformable contours algorithms to segmenting the carotid lumen. Journal of Electronic Imaging 23(2):023,006–023,006

[11] Jaworek-Korjakowska J, Tadeusiewicz R (2015) Design of a teledermatology system to support the consultation of dermoscopic cases using mobile technologies and cloud platform. Bio–Algorithms and Med–Systems 11(1):53–58

[12] Khan MAU, Niazi MKK, Khan MA, Ibrahim MT (2007) Endothelial cell image enhancement using non-subsampled image pyramid. Information Technology Journal 6(7):1057–1062
[13] Mahzoun M, Okazaki K, Mitsumoto H, Kawai H, Sato Y, Tamura S, Kani K (1996) Detection and complement of hexagonal borders in corneal endothelial cell image. Medical Imaging Technology 14(1):56–69
[14] Mazurek P, Oszutowska-Mazurek D (2014) From the slit-island method to the ising model: Analysis of irregular grayscale objects. International Journal of Applied Mathematics and Computer Science 24(1):49–63
[15] Nadachi R, Nunokawa K (1992) Automated corneal endothelial cell analysis. In: Computer-Based Medical Systems, 1992. Proceedings., Fifth Annual IEEE Symposium on, IEEE, pp 450–457
[16] Nurzynska K, Haraszczuk R (2012) Detection and normalization of blown-out illumination areas in grey-scale images. In: Advances in Visual Computing, Springer, pp 282–291
[17] Piorkowski A (2016) A statistical dominance algorithm for edge detection and segmentation of medical images. In: Information Technologies in Medicine, Advances in Intelligent Systems and Computing, vol 471, Springer, pp 3–14
[18] Piorkowski A, Gronkowska-Serafin J (2015) Towards precise segmentation of corneal endothelial cells. In: Bioinformatics and Biomedical Engineering, Lecture Notes in Computer Science, vol 9043, pp 240–249
[19] Ruggeri A, Scarpa F, De Luca M, Meltendorf C, Schroeter J (2010) A system for the automatic estimation of morphometric parameters of corneal endothelium in alizarine red-stained images. British Journal of Ophthalmology 94(5):643–647
[20] Saeed K, Tabędzki M, Rybnik M, Adamski M (2010) K3M: A universal algorithm for image skeletonization and a review of thinning techniques. International Journal of Applied Mathematics and Computer Science 20(2):317–335
[21] Sanchez-Marin F (1999) Automatic segmentation of contours of corneal cells. Computers in Biology and Medicine 29(4):243–258
[22] Selig B, Vermeer KA, Rieger B, Hillenaar T, Hendriks CLL (2015) Fully automatic evaluation of the corneal endothelium from in vivo confocal microscopy. BMC medical imaging 15(1):1